Hindawi Publishing Corporation
Journal of Chemistry
Volume 2013, Article ID 973160, 10 pages
http://dx.doi.org/10.1155/2013/973160

Research Article

Catalytic Performance of Fe-Mn/SiO_2 Nanocatalysts for CO Hydrogenation

Mostafa Feyzi, Shirin Nadri, and Mohammad Joshaghani

Faculty of Chemistry, Razi University, P.O. Box 67149, Kermanshah 6714967346, Iran

Correspondence should be addressed to Mostafa Feyzi; dalahoo2011@yahoo.com

Received 4 June 2012; Revised 31 July 2012; Accepted 10 August 2012

Academic Editor: Albert Demonceau

A series of x(Fe, Mn)/SiO_2 nanocatalysts (x = 5, 10, 15, 20, 25, and 30 wt.%) were prepared by sol-gel method and studied for the light olefins production from synthesis gas. It was found that the catalyst containing 20 wt.% (Fe, Mn)/SiO_2 is an optimal nano catalyst for production of C_2–C_4 olefins. Effects of sulfur treatment on the catalyst performance of optimal catalyst have been studied by espousing different volume fractions of H_2S in a fixed bed stainless steel reactor. The results show that the catalyst treated with 6 v% of H_2S had high catalytic performance for C_2–C_4 light olefins production. The best operational conditions were H_2/CO = 3/2 molar feed ratio at 260°C and GHSV = 1100 h^{-1} under 1 bar total pressure. Characterization of catalysts was carried out using X-ray diffraction (XRD), scanning electron microscopy (SEM), transmission electron microscopy (TEM), and surface area measurements.

1. Introduction

Since initial introduction of Fischer-Tropsch synthesis (FTS), increasing concentration has been made for the increasing of advantages as well as drawback reduction of this potentially commercial process. One of the best approaches to improve the selectivity toward viably more important products involves the use of a supported bimetallic catalyst [1]. Using this approach, selective production of petrochemical feed stocks such as ethylene, propylene, and butylenes (C_2–C_4 light olefin) directly from syngas is hoped to be attainable [2, 3]. Due to opinion of high activity and selectivity as well as the cost problems, iron-based catalysts are the catalysts of choice. The other metal partner is typically manganese or cobalt. A high olefin selectivity for Fe-Mn catalysts has been reported due to formation of iron-manganese oxides and carbide phases [3, 4]. Recent studies show that primary α-olefin products of the FTS were subjected to afterward reactions on iron surface [5–8]. Sulfur treatment is the subject of contrast results. Barrault et al. [9] studied the poisoning of cobalt and iron catalysts by sulfur and observed a decrease in catalytic activity and a propensity for forming lower olefins. Similar results are reported by Kitzelmann and Vielstich [10] who used a K_2S to achieve a light poisoning of Fe and Co catalysts. The methane selectivity was reduced by 50% and the lower olefin selectivity was increased by ≈10%. Due to accumulation and deactivating times, most of the researches on sulfur poisoning were done using exaggerated sulfur levels of the syngas. In contrast, there are some recent reviews [11, 12] and reports highlighting the advantageous effects of sulfur on both iron [13, 14] and other active metals [15–20]. It has been demonstrated that a small amount of sulfur species on the catalyst surface could be associated with improved FTS activity and enhanced olefin selectivity. It was also reported that the activity was only slightly lowered by this treatment. Li and Coville have observed a decrease in methanation for Co/TiO_2 catalyst [21, 22]. Anderson et al. found that selectivity toward light hydrocarbons products increased with increasing sulfur content of alkali-promoted iron catalysts and [23–27]. Stenger and Satterfield [26] reported a 60% increase in the activity of a fused magnetite catalyst after exposure to synthesis gas containing H_2S.

Herein, we investigated the role of H_2S-treated catalyst on decreasing of methane and increasing the C_2–C_4 olefins in products. We also reported the optimization process and effects of operational conditions on the catalytic performance

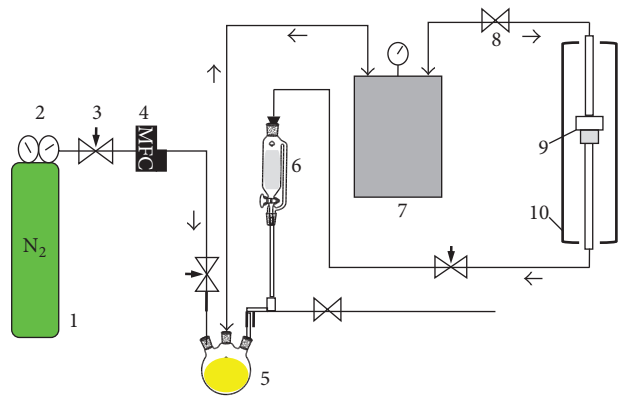

Figure 1: Schematic representation of the H_2S production and treating system. 1: Gas cylinders, 2: pressure regulators, 3: needle valves, 4: mass flow controllers (MFCs), 5: reflux flask, 6: dropping funnel, 7: tank, 8: ball valves, 9: tubular reactor and catalyst bed, 10: tubular Furnace.

of an optimal catalyst. Characterization of catalysts was carried out using X-ray diffraction (XRD), scanning electron microscopy (SEM), transmission electron microscopy (TEM), and surface area measurements.

2. Experimental

All chemical reagents and solvents were analytical grade and purchased from Fluka and Merck. The specific surface area, the total pore volume, and the mean pore diameter were measured using a NOVA 2200 instrument. The XRD patterns of the precursor and calcined samples were recorded on a Philips X' Pert (40 kV, 30 mA) X-ray diffractometer using a Cu Kα radiation source (λ = 1.542 Å) and a nickel filter. The TEM investigations were carried out using an H-7500 (120 kV). The morphology of catalyst and precursor was observed by means of S-360 scanning electron microscopy.

2.1. Catalyst Preparation. $Fe(NO_3)_3{\cdot}9H_2O$ and $Mn(NO_3)_2{\cdot}4H_2O$ (Fe/Mn molar ratio is 3/1 [28]), tetraethyl orthosilane were dissolved separately in ethanol at 60°C and mixed together. An ethanolic solution of oxalic acid ($H_2C_2O_4{\cdot}2H_2O$) (10 wt% excess) was added gradually under constancy stirring (300 rpm) to give transparent monolithic gel. The formation of iron and manganese oxalate was associated with the formation of nitric acid which contributed to the acidity of the medium (pH = 1 ± 0.1). The obtained material containing iron and manganese oxalate was slowly dried at 100°C in oven, powdered, and calcined at 500°C for 6 h in air atmosphere and heating rate of 2°C min^{-1}.

2.2. H_2S Treats the Catalysts. H_2S-treating experiments were performed in a gas circulation system composed of H_2S generator and sulfur treatment reactor parts (Figure 1). The catalyst containing 20 wt.% (Fe, Mn)/SiO_2 was treated with different H_2S volume fraction at 200°C and 1 bar for 5 h. The treated catalysts then were subjected to FTS production of light olefins under same reaction conditions (H_2/CO = 2/1, GHSV = 1000 h^{-1}, P = 1 bar at 250°C).

2.3. Catalyst Testing. Catalysts were tested in a fixed bed stainless steel reactor at different operational conditions (Figure 2). The meshed catalyst (0.5 g) was diluted with similar granules of quartz beads (1.0 g) and held in the middle of the reactor (30 cm length and internal diameter 6 mm). All catalysts were activated on-line (reduced) for a 10 h period in pure hydrogen (1 bar) at a temperature of 400°C and space velocity of 800 h^{-1}. Reactant and stream products were analyzed on-line using a Varian Star 3600CX gas chromatograph equipped with a thermal conductivity detector (TCD) and a chromosorb column. The heavy hydrocarbon products were analyzed off-line using a Varian CP 3800 gas chromatograph with a Petrocol Tm DH100 fused silica capillary column and a flame ionization detector (FID). The conversion percentage of CO was based on the fraction of CO that formed carbon-containing products according to

$$\text{CO conversion } (\%) = \frac{\sum n_i M_i}{M_{\text{CO}}} \times 100, \quad (1)$$

where n_i is the number of carbon atoms in product i, M_i is the weight percentage of product i, and M_{CO} is the percentage of CO in the syngas feed.

The selectivity (S) toward product i is based on the total number of carbon atoms in the product and is therefore defined as

$$S_i\,(\%) = \frac{n_i M_i}{\sum n_i M_i} \times 100. \quad (2)$$

3. Results and Discussion

3.1. Catalytic Performance

3.1.1. Effect of Metals Loading. Catalysts of the formula x(Fe, Mn)/SiO_2 were prepared with different x loadings (x = 5, 10, 15, 20, 25, and 30 wt.% based on the support weight) and tested for the FTS under same reaction conditions (H_2/CO = 2/1, GHSV = 1000 h^{-1}, P = 1 bar at 250°C). The CO conversion and products selectivity in the steady state condition

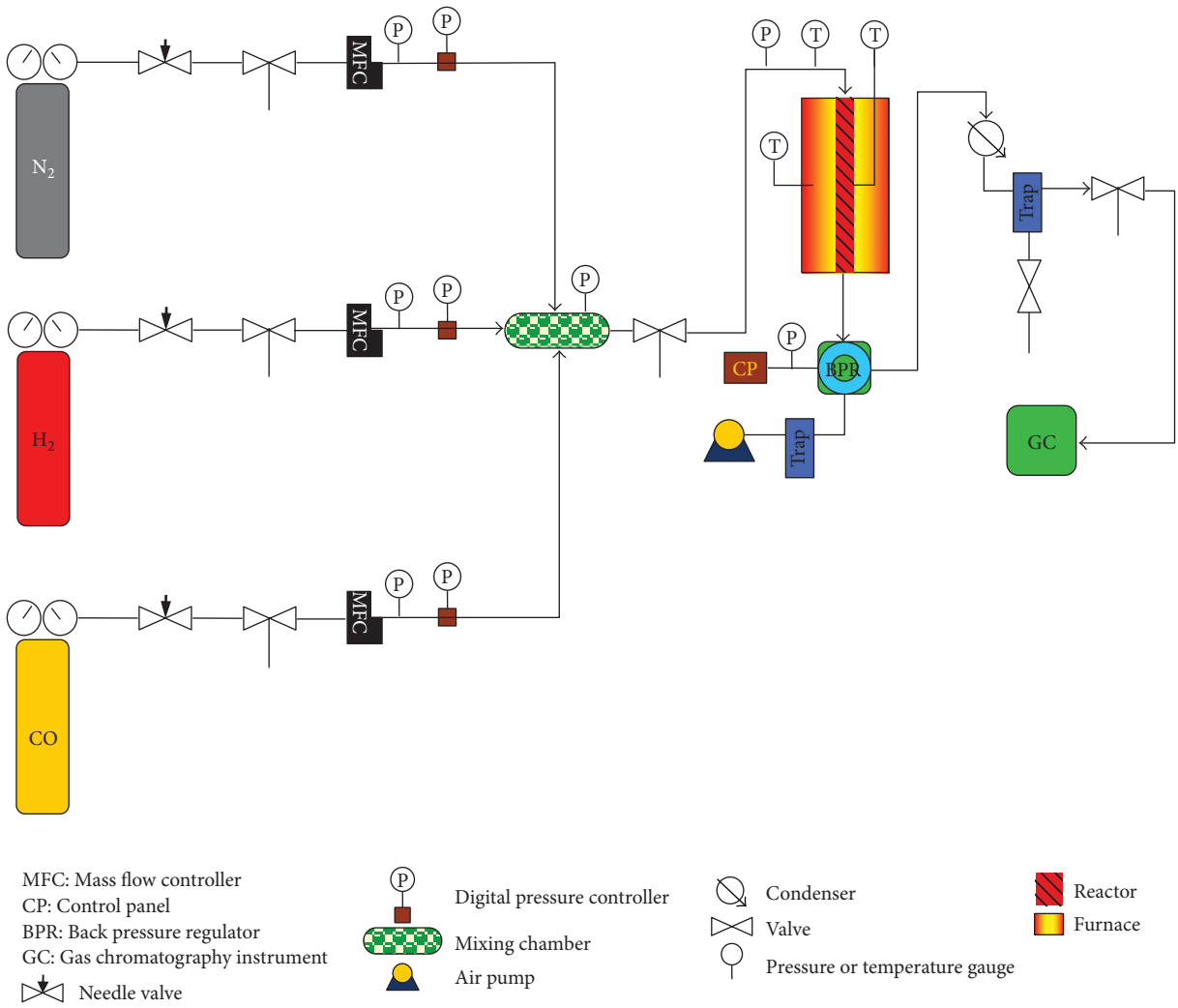

Figure 2: Schematic representation of the catalyst performance system.

(the time required to attain steady-state condition was about 10 h) were summarized in Table 1. According to the results, the catalyst containing 20 wt.% (Fe, Mn)/SiO_2 has the highest selectivity towards C_2–C_4 olefins and the lowest selectivity with respect to methane and CO_2. Therefore, this catalyst was chosen as the optimal catalyst for the conversion of synthesis gas to light olefins. Characterization studies were carried out using various techniques for both the precursors and calcined catalysts. SEM images show a few differences in morphology of precursor and calcined catalysts (Figure 3). The catalyst precursor seems to have relatively larger agglomerations of particles than the calcined catalyst. Characterization studies were carried out using XRD technique for the 20 wt.% (Fe, Mn)/SiO_2 calcined catalysts (Figure 4). The actual identified phases for this catalyst were Fe_3O_4 (cubic), SiO_2 (hexagonal), Mn_2O_3 (cubic), and Fe_2O_3 (rhombohedral). The particle size was determined from the half width of the most intense peak of the diffraction pattern around $2\theta = 33.4$ using the Scherrer equation [29], $d = K\lambda/B\cos\theta$, where d is the mean crystallite diameter, K has an assumed value of 0.9, λ is the X-ray wave length (1.54 Å), and B is the width of the diffraction peak at half maximum. The catalysts containing 20 wt.% (Fe,Mn)/SiO_2 have particle sizes of about 35 nm. The catalyst containing 20 wt.% (Fe, Mn)/SiO_2 was characterized with TEM [30] (Figure 5). As shown in Figure 5, the particle sizes are from 25–40 nm. This result conform with obtained results that was studied by using the Scherrer equation.

3.2. Process for H_2S Treatment of the Catalyst. As Figure 1 shows, the system composed of two parts, H_2S generator and sulfur treatment reactor. The H_2S was produced on addition of H_2SO_4 (from dropping funnel 6) to a flask containing $Na_2S{\cdot}xH_2O$ (flask 5) and then was mixed with N_2 and conducted to a stainless steel reactor. The carrier gas containing desired volume fraction of H_2S ($V_{H_2S}/(V_{H_2S} + V_{N_2})$) was passed over the meshed catalyst (1.0 g) held in the middle of a fixed bed stainless steel reactor ($T = 200^{\circ}C$ and $P = 1$ bar for 5 h). Before H_2S treatment of the catalyst, the system should be exposed to the stream of pure N_2 for 30 min to eliminate the oxygen.

Table 1: Effect of loading of (Fe-Mn) on the catalytic performance of catalysts.

wt.% (Fe, Mn)		5	10	15	20	25	30
CO conversion (%)		43.7	46.4	52.6	62.8	65.7	60.2
Product selectivity (%)	CH_4	31.4	29.1	25.7	24.3	26.3	28.5
	$\sum C_2$–C_4	46.9	46.7	49	52	52.8	48.3
	C_2H_6	6.8	6.4	6.2	5.7	6.5	7.5
	C_2H_4	11.1	12.8	12.8	14.4	12.7	10.4
	C_3H_8	7.3	6.7	7.0	6.7	7.9	8.6
	C_3H_6	8.4	7.1	8.3	9.5	8.6	7.5
	C_4H_{10}	6.8	6.9	6.3	7.3	8.0	6.2
	C_4H_8	6.5	6.8	8.4	9.4	9.1	8.1
	$\sum C_5$–C_9	8.3	9.5	8.7	9.2	10.4	11.1
	C_{10}+	6.9	8.7	11.4	8.9	5.1	5.8
	CO_2	6.5	6.0	5.2	4.6	5.4	6.3
Olefin/parrafin ratio	C_2–C_4	1.2	1.3	1.5	1.7	1.4	1.2
	C_2	1.6	2	2.1	2.5	2.0	1.4
	C_3	1.2	1.1	1.2	1.4	1.1	0.9
	C_4	1.0	0.1	1.3	1.3	1.1	1.3

Reaction conditions: $H_2/CO = 2/1$, GHSV = 1000 h^{-1}, and P = 1 bar at 250°C.

Table 2: Effect of different H_2S volume fractions on the catalytic performance of catalyst[a].

H_2S volume fractions[b]		0.02	0.04	0.06	0.08	0.1	0.12
CO conversion (%)		64.4	65.2	67.4	65.7	58.4	43.5
Product selectivity (%)	CH_4	23.4	21.1	18.5	17.6	7.01	17.0
	$\sum C_2$–C_4	53.5	54.5	56.8	56.5	52.8	53.1
	C_2H_6	5.8	5.7	4.9	6.8	6.7	10.4
	C_2H_4	15.1	15.2	17.7	14.2	13.2	11.3
	C_3H_8	8.3	8.5	8.4	8.9	8.5	9.6
	C_3H_6	8.4	9.1	9.5	8.6	5.7	6.4
	C_4H_{10}	5.0	5.0	4.1	7.7	9.3	8.1
	C_4H_8	10.9	11.0	12.2	10.3	9.4	7.3
	$\sum C_5$–C_9	10.2	10.5	10.5	12.0	13	11.0
	C_{10}+	9.4	10.5	10.9	10.6	12.7	13.5
	CO_2	3.5	3.4	3.3	3.3	4.5	5.4
Olefin/parrafin ratio	C_2–C_4	1.8	1.8	2.3	1.4	1.2	0.9
	C_2	2.6	2.7	3.6	2.1	2.0	1.1
	C_3	1.0	1.1	1.1	1.0	0.7	0.7
	C_4	0.6	2.2	3.0	1.3	1.0	0.9

[a] Reaction conditions: $H_2/CO = 2/1$, GHSV = 1000 h^{-1}, and P = 1 bar at 250°C.
[b] H_2S volume fractions = $V_{H_2S}/(V_{H_2S} + V_{N_2})$.

3.2.1. Effect of H_2S Volume Fraction. The catalyst containing 20 wt.% (Fe, Mn)/SiO_2 was treated with different H_2S volume fraction at 200°C and 1 bar for 5 h and then the treated catalysts were subjected to FTS production of light olefins under same reaction conditions ($H_2/CO = 2/1$, GHSV = 1000 h^{-1}, P = 1 bar at 250°C). The results show the highest total selectivity respect to C_2–C_4 light olefins products (C_2–C_4 olefins/C_2–C_4 paraffin = 2.26) as well as the least CH_4 and CO_2 selectivities were achieved using 6/100 H_2S volume fraction (Table 2). Higher volume fractions led to less total CO conversion which is a drawback in the industrially point of view. Thus, the effects of sulfur strongly depend on the S loading, possibly because different catalyst functions are affected by sulfur.

Table 3: N_2 adsorption-desorption measurements of iron-manganese catalyst treated with H_2S.

H_2S volume fractions[a]	Specific surface area ($m^2\ g^{-1}$)	Pore diameter (Å)	Pore volume ($cm^3\ g^{-1}$)
—	205.7	46.4	0.31
2/100	225.6	47.9	0.37
4/100	228.5	49.3	0.39
6/100	233.5	53.2	0.42
8/100	228.3	51.5	0.39
10/100	219.7	50.4	0.38
12/100	213.9	47.9	0.34

[a] H_2S volume fractions = $V_{H_2S}/(V_{H_2S} + V_{N_2})$.

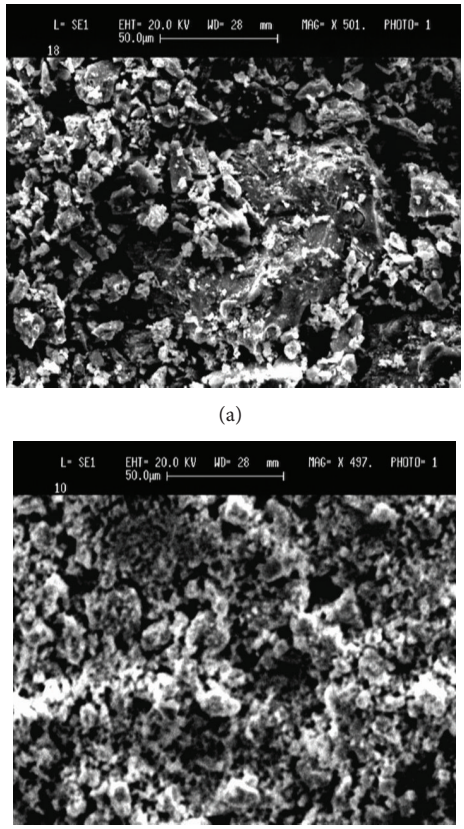

(a)

(b)

Figure 3: SEM images of precursor (a) and calcined catalyst containing 20 wt.% (Fe, Mn)/SiO_2.

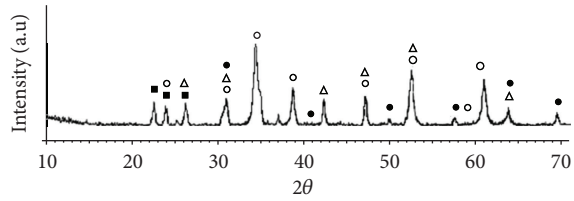

Figure 4: XRD patterns of the calcined catalyst containing 20 wt.% (Fe, Mn)/SiO_2: ● Fe_3O_4 (cubic), ◦ Fe_2O_3 (rhombohedral), ▲ Mn_2O_3 (cubic), and ■ SiO_2 (hexagonal).

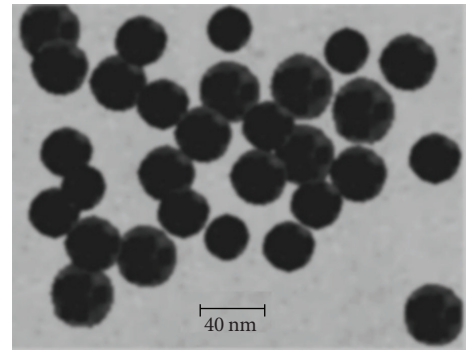

Figure 5: TEM image of calcined catalyst containing 20 wt.% (Fe, Mn)/SiO_2.

A possible reaction proposed by Van der Kraan et al. [27] may be accounted for the advantages of sulfur treatment of iron-based FT catalysts (3):

$$Fe_2O_3 \cdot H_2O + 3H_2S \longrightarrow 2FeS + 4H_2O + S \quad (3)$$

Partially sulfidation of the catalyst gives the sulfide phases which act as support and hence maintains the dispersion of the iron centers. Vacancies created by the loss of H_2O and sulfur also increase the porosity of the sulfide salt of catalysts.

Surface area of the sulfur-treated and untreated catalysts was determined using N_2 absorption desorption. The results show significant effects of sulfur treatment on porosity and specific surface area of catalyst (Table 3). The results show that specific surface area increases with increasing the H_2S volume fraction until to 6 v%. The data could imply that the S increases the dispersion of the Fe and Mn which might be a reason for the better catalytic performance of the above catalyst [27, 28, 31]. It can be seen from Table 3 that sulfur treatment in excess of 6 v% resulted in a decrease in the specific surface area and CO conversion. According to Table 2, it seems that it is the specific surface area, pore volume, and pore size distribution are dependent to sulfur treatment.

The H_2S-treated (6 v%) catalyst was subjected to XRD characterization before and after catalyst performance test, and the corresponding XRD patterns are presented in Figure 6. Before the performance test, the XRD pattern shows the presence of $Fe_{1-x}S$ (hexagonal) phase in addition to

Table 4: Effect of different H_2/CO feed ratio on the catalytic performance of catalyst.

H_2/CO molar ratio		1/1	2/1	3/2	3/1
CO conversion (%)		58.7	67.4	70.8	58.3
Product selectivity (%)	CH_4	19.8	18.5	16.4	20.4
	$\sum C_2$–C_4	52.7	56.8	60.9	50.4
	C_2H_6	6.3	4.9	6.5	8.7
	C_2H_4	15.2	17.7	18.2	13.3
	C_3H_8	7.6	8.4	7.4	7.2
	C_3H_6	8.0	9.5	10.4	7.1
	C_4H_{10}	6.1	4.1	5.3	6.5
	C_4H_8	9.5	12.2	13.1	7.6
	$\sum C_5$–C_9	12.8	10.5	11.2	12.3
	C_{10}+	9.4	10.9	8.5	10.4
	CO_2	5.3	3.3	3.0	6.5
Olefin/parrafin ratio	C_2–C_4	1.6	2.3	2.2	1.3
	C_2	2.4	3.6	2.8	1.5
	C_3	1.1	1.1	1.4	1.0
	C_4	0.5	3.0	2.5	1.2

Reaction conditions: GHSV = 1000 h^{-1}, P = 1 bar at 250°C.

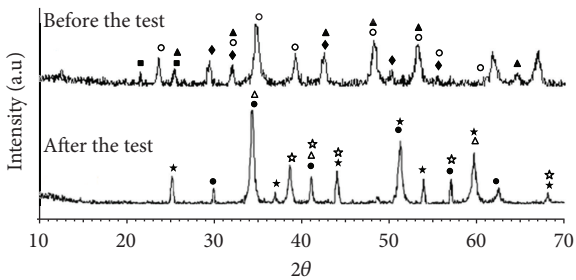

Figure 6: XRD patterns of the sulfur-treated catalysts (0.6%) before and after test: ◆ $Fe_{1-x}S$ (hexagonal), ● Fe_3O_4 (cubic), ◦ Fe_2O_3 (rhombohedral), ▲ Mn_2O_3 (cubic), △ MnO (cubic), ∎ SiO_2 (hexagonal), ⋆ FeC (orthorhombic), and ☆ Fe_2C (hexagonal).

Fe_2O_3 (rhombohedral), Mn_2O_3 (cubic), and SiO_2 (hexagonal). These patterns disappear after the performance test and instead another pattern that belongs to Fe_3O_4 (cubic), MnO (cubic), and carbide phases FeC and Fe_2C appears. The results show that the sulfide phase has been removed during the reaction. In addition, metallic iron is rapidly converted to iron carbide during the reaction which may be subjected to further oxidation into Fe_3O_4. It is well known that the iron carbides phases are active for FTS and oxidic species are responsible for production of olefins [32–34].

3.3. Effect of Operational Conditions. One of the other major factors which have a marked effect on the catalytic performance of a catalyst is the operating conditions. For optimizing of the reaction conditions in this study, the effects of operating conditions such as H_2/CO feed molar ratios, GHSV, reaction temperatures, and reactor total pressures were examined to investigate the catalyst stability and its performance for the light olefins production.

3.3.1. Effect of H_2/CO Molar Feed Ratio. The influence of the H_2/CO molar feed ratio on the steady state catalytic performance of the catalyst treated with 6 v% of H_2S was investigated for the FTS at 250°C, GHSV = 1000 h^{-1}, and atmospheric pressure. The CO conversion and light olefin products selectivity percent are shown in Table 4. The results showed that with variation in H_2/CO molar feed ratios from 1/1 to 3/1, different selectivity with respect to C_2–C_4 light olefins was obtained. Among them, for H_2/Com = 3/2 (GHSV = 1000 h^{-1}), the total selectivity of C_2–C_4 light olefins was the highest while, the CH_4 and CO_2 selectivity was the least. Therefore, the H_2/CO = 3/2 ratio was chosen as the optimum ratio for conversion of the syngas to C_2–C_4 olefins over the 20 wt.% (Fe, Mn)/SiO_2 nanocatalyst treated with 6 v% of H_2S.

3.3.2. Effect of Gas Hourly Space Velocity (GHSV). To obtain a better understanding of the factors affecting the catalytic performance of 20 wt.% (Fe, Mn)/SiO_2 nanocatalyst treated with 6 v% of H_2S, a series of experiments were carried out at different GHSV from 800 to 1300 h^{-1} under the reaction conditions (H_2/CO = 3/2, P = 1 bar at 250°C), and the results are presented in the Table 5. The CO conversion increased with increasing space velocity and reached a maximum CO conversion of 72% for space velocity of 1100 h^{-1} and then decreased with further increasing of space velocity. At the same time, methane and CO_2 selectivity decreased till space velocity of 1100 h^{-1} then increases markedly. Madon and Taylor [35] studied the effect of space velocity on the olefins and paraffins selectivity for Ru catalyst and

Table 5: Effect of different GHSV on the catalytic performance of catalyst[a].

GHSV (h^{-1})		800	900	1000	1100	1200	1300
CO conversion (%)		67.1	68.7	70.8	72.0	65.3	57.3
Product selectivity (%)	CH_4	18.7	17.3	16.4	15.3	17.2	19.7
	$\sum C_2$–C_4	55.2	52.9	60.9	64	57.1	51.5
	C_2H_6	8.8	7.3	6.5	7.4	6.7	7.9
	C_2H_4	13.5	14.5	18.2	18.9	15.7	10.3
	C_3H_8	7.9	6.3	7.4	7.1	7.8	9.8
	C_3H_6	8.6	8.9	10.4	11.5	10.3	10.2
	C_4H_{10}	6.3	4.6	5.3	4.6	6.4	5.9
	C_4H_8	10.1	11.3	13.1	14.5	10.2	7.4
	$\sum C_5$–C_9	12.9	13.7	11.2	10.1	12.5	12.9
	C_{10}+	8.6	12.1	8.5	8.1	9.2	11.7
	CO_2	4.6	4.0	3.0	2.5	4.0	4.2
Olefin/parrafin ratio	C_2–C_4	1.4	1.9	2.2	2.4	1.7	1.2
	C_2	1.5	2.0	2.8	2.6	2.3	1.3
	C_3	1.1	1.4	1.4	1.6	1.3	1.0
	C_4	0.4	2.5	2.5	3.2	1.6	1.3

Reaction conditions: $H_2/CO = 3/2$, $P = 1$ bar at 250°C.

Table 6: Effect of different reaction temperature on the catalytic performance of catalyst.

Temperature (°C)		220	230	240	250	260	270	280	290
CO conversion (%)		56.3	61.6	67.9	72.0	73.7	75.2	77.2	79.1
Product selectivity (%)	CH_4	14.1	14.9	15.6	15.3	15.3	17.5	21.9	23.8
	$\sum C_2$–C_4	57.5	57	58	64	65.6	59.5	54.6	51.9
	C_2H_6	9.8	6.6	7.1	7.4	6.5	10.2	11.9	12.6
	C_2H_4	13.1	14.8	16.5	18.9	20.4	11.2	8.6	7.1
	C_3H_8	6.8	6.3	6.8	7.1	6.5	11.0	9.3	8.1
	C_3H_6	9.3	9.9	10.1	11.5	12.1	9.5	9.7	8.3
	C_4H_{10}	7.4	6.8	5.1	4.6	5.2	7.4	8.3	9.1
	C_4H_8	11.1	12.6	12.9	14.5	14.9	10.2	6.8	6.7
	$\sum C_5$–C_9	11.2	13.5	12.7	10.1	9.1	12.9	8.4	7.3
	C_{10}+	12.4	11.2	10.1	8.1	7.2	14.5	10.2	7.4
	CO_2	4.8	3.4	3.1	2.5	2.3	5.6	5.8	9.6
Olefin/parrafin ratio	C_2–C_4	1.4	1.9	2.1	2.4	2.6	1.1	0.9	0.7
	C_2	1.3	2.2	2.3	2.6	3.1	1.0	0.7	0.6
	C_3	1.4	1.6	1.5	1.6	1.9	0.9	1.0	1.0
	C_4	0.4	2.5	2.5	3.2	2.9	1.4	0.8	0.7

Reaction conditions: $H_2/CO = 3/2$, GHSV = 1100 h^{-1}, and $P = 1$ bar.

found that the olefin selectivity increased with increasing space velocity. According to the results in Table 5, at the ranges of 800–1100 h^{-1}, significant increasing on light olefins selectivity was observed. It is apparent that in GHSV = 1100 h^{-1} the selectivity for C_2–C_4 light olefins was increased. Therefore, in this study, GHSV = 1100 h^{-1} is considered to be better GHSV at 250°C, because in this GHSV a high CO conversion and total selectivity of light olefins products and low CH_4 and CO_2 selectivity were observed. These results indicate that the GHSV is a parameter of crucial importance on the catalytic performance of iron-manganese catalysts for hydrogenation of CO.

3.3.3. Effect of Reaction Temperature. The effect of reaction temperature on the catalytic performance of the 20 wt.% (Fe, Mn)/SiO_2 nanocatalyst treated with 6 v% of H_2S was

Table 7: Effect of different total reaction pressure on the catalytic performance of catalyst.

Pressure (bar)		1	2	3	4	5	6	7	8	9	10
CO conversion (%)		73.7	67.5	66.3	66.0	66.0	61.5	62.0	62.3	61.1	58.9
Product selectivity (%)	CH_4	15.3	14.7	14.3	14.0	13.7	12.8	11.7	10.6	10.3	10.3
	$\sum C_2$–C_4	65.5	62.1	57	53.3	50.4	48.5	45.2	39.5	37.2	33.4
	C_2H_6	6.5	5.8	5.1	5.4	5.6	5.4	5.2	5.4	4.7	4.2
	C_2H_4	20.4	18.3	14.2	12.1	8.2	7.4	6.5	6.1	5.8	5.5
	C_3H_8	6.5	4.1	4.7	4.9	5.2	5.2	6.1	5.5	5.2	4.7
	C_3H_6	12.1	11.7	11.4	10.0	8.7	7.8	6.6	5.9	6.3	5.5
	C_4H_{10}	5.2	5.8	6.3	6.8	6.9	8.4	7.4	6.3	5.8	5.4
	C_4H_8	14.9	16.4	15.3	14.1	15.8	14.3	13.4	10.3	9.4	8.1
	$\sum C_5$–C_9	9.1	11.3	15.4	16.9	18.7	19.6	21.6	24.7	26.4	27.1
	C_{10}+	7.2	9.5	10.9	12.3	13.7	14.3	16.5	20.0	20.6	23.5
	CO_2	2.3	2.4	2.4	3.5	3.5	4.8	5.0	5.2	5.5	5.7
Olefin/parrafin ratio	C_2–C_4	2.6	3.0	2.5	2.1	1.9	1.6	1.4	1.3	1.4	1.3
	C_2	3.1	3.2	2.8	2.2	1.5	1.4	1.3	1.1	1.2	1.3
	C_3	1.9	2.9	2.4	2.0	1.7	1.5	1.1	1.0	1.2	1.2
	C_4	2.9	2.8	2.4	2.1	2.3	1.7	1.6	0.7	1.6	1.5

Reaction conditions: $H_2/CO = 3/2$, GHSV = 1100 h^{-1}, and $T = 260^{\circ}C$.

studied at a range of temperatures between 220–290°C under the same reaction conditions (P = 1 bar, $H_2/CO = 3/2$, and GHSV = 1100 h^{-1}), and the results are presented in the Table 6. The results show that for the reaction temperature at 260°C, the total selectivity of light olefins products was the highest. In addition, the CO conversion increases with increasing the operating temperature. In the same way, it has been reported that at low reaction temperatures, the conversion percentage of CO is low and so it causes a low catalytic performance [9]. On the other hand, increasing the reaction temperature leads to increasing of methane as an unwanted product. Therefore, in this study, 260°C is considered the optimum operating temperature. These results indicate that the reaction temperature is a parameter of crucial importance in the catalytic performance of iron-manganese catalyst for hydrogenation of CO.

3.3.4. Effects of Total Pressure. A series of experiments were carried out to investigate the performance of the 20 wt.% (Fe, Mn)/SiO_2 nanocatalysts treated with 6 v% of H_2S during variation of total pressure in the range of 1–10 bar, at the optimal reaction conditions of $H_2/CO = 3/2$, GHSV = 1100 h^{-1}, and 260°C (Table 7). The results indicate that at the total pressure of 1 bar, the optimal catalyst showed a high selectivity respect to C_2–C_4 light olefins. It is also apparent that the C_5–$C_9$and C_{10}+ selectivities increase with increasing the pressure [36]. The results also indicate that the CO conversion and the total selectivity with respect to C_2–C_4 light olefins decrease with increasing the pressure. Increase in the selectivity of higher molecular weight hydrocarbons of Fe-Mn catalyst upon increasing the pressure can be explained by the increased concentration of α-olefins and readsorption and chain initiation of these primary products on catalyst surface which lead to the ultimate desorption of these α-olefins as larger products.

Hence, because of high CO conversion and higher total selectivity with respect to C_2–C_4 olefins at the total pressure of 1 bar, this pressure was chosen as the optimum pressure.

4. Conclusions

In conclusion, it is found that the activity and selectivity of the catalyst are affected by the level of sulfur adsorbed on the catalyst, and the catalyst treated with 6 v% of H_2S showed the best catalytic performance for light olefins production. The operational conditions such as H_2/CO molar feed ratio, gas hourly space velocity (GHSV), reaction temperature, and reaction total pressure were very effective and the optimal operating conditions for production of light olefins were found to be 260°C with molar feed ratio of $H_2/CO = 3/2$ (GHSV = 1100 h^{-1}) under the total pressure of 1 bar. The optimal nanocatalyst treated with 6 v% of H_2S was found to be superior to the other catalysts in terms of better C_2–C_4 selectivity in the FTS products and higher olefin/paraffin ratio (2.6). In addition, methane formation by using this modified catalyst was suppressed, which caused decreasing of methane selectivity from 24.3 to 15.8% at 260°C with molar feed ratio of $H_2/CO = 3/2$ (GHSV = 1100 h^{-1}) under the total pressure of 1 bar.

Acknowledgments

The authors thank the Iran National Science Foundation (INSF) for financial support and Razi University Research Council for partial support of this work.

References

[1] S. L. González-Cortés, S. M. A. Rodulfo-Baechler, A. Oliveros et al., "Synthesis of light alkenes on manganese promoted iron and iron-cobalt Fischer-Tropsch catalysts," *Reaction Kinetics and Catalysis Letters*, vol. 75, no. 1, pp. 3–12, 2002.

[2] F. R. Van den Berg, M. W. J. Crajé, A. M. Van der Kraan, and J. W. Geus, "Reduction behaviour of Fe/ZrO_2 and $Fe/K/ZrO_2$ Fischer-Tropsch catalysts," *Applied Catalysis A*, vol. 242, no. 2, pp. 403–416, 2003.

[3] F. Tihay, A. C. Roger, A. Kiennemann, and G. Pourroy, "Fe–Co based metal/spinel to produce light olefins from syngas," *Catalysis Today*, vol. 58, no. 4, pp. 263–269, 2000.

[4] R. Malessa and M. Baerns, "Iron/manganese oxide catalysts for Fischer-Tropsch synthesis: activity and selectivity," *Industrial and Engineering Chemistry Research*, vol. 27, no. 2, pp. 279–283, 1988.

[5] M. Feyzi, M. M. Khodaei, and J. Shahmoradi, "Effect of preparation and operation conditions on the catalytic performance of cobalt-based catalysts for light olefins production," *Fuel Processing Technology*, vol. 93, no. 1, pp. 90–98, 2012.

[6] P. Villeger and G. R. Leclercq, "Synthesis of hydrocarbons from carbon monoxide. 1. Activity and selectivity of nickel-based bimetallic catalysts," *Chemical Abstracts*, vol. 93, no. 170786, 1980.

[7] D. J. Duvenhage and N. J. Coville, "$Fe–Co/TiO_2$ bimetallic catalysts for the Fischer-Tropsch reaction I. Characterization and reactor studies," *Applied Catalysis A*, vol. 153, no. 1-2, pp. 43–67, 1997.

[8] C. Cabet, A. C. Roger, A. Kiennemann, S. Läkamp, and G. Pourroy, "Synthesis of new Fe-Co based metal/oxide composite materials: application to the Fischer-Tropsch synthesis," *Journal of Catalysis*, vol. 173, no. 1, pp. 64–73, 1998.

[9] J. Barrault, C. Forquy, and V. Perrichon, "Effects of manganese oxide and sulphate on olefin selectivity of iron supported catalysts in the Fischer-Tropsch reaction," *Applied Catalysis*, vol. 5, no. 1, pp. 119–125, 1983.

[10] D. Kitzelmann and W. Vielstich, "In-situ study of the primary reactions in the hydrogenation of CO on Fe-catalysts Fischer-Tropsch synthesis," *Journal of Physical Chemistry*, vol. 112, pp. 215–233, 1978.

[11] C. H. Bartholomew, P. K. Agrawal, and J. R. Katzer, "Sulfur poisoning of metals," *Advances in Catalysis*, vol. 31, no. C, pp. 135–242, 1982.

[12] J. Barbier, E. Lamy-Pitara, P. Marecot, J. P. Boitiaux, J. Cosyns, and F. Verna, "Role of sulfur in catalytic hydrogenation reactions," *Advances in Catalysis*, vol. 37, no. C, pp. 279–318, 1990.

[13] A. L. Chaffee, I. Campbell, and N. Valentine, "Sulfur poisoning of Fischer-Tropsch synthesis catalysts in a fixed-bed reactor," *Applied Catalysis*, vol. 47, no. 2, pp. 253–276, 1989.

[14] W. L. van Dijk, J. W. Niemantsverdriet, A. M. van dar Kraan, and H. S. van der Baan, "Effects of manganese oxide and sulphate on the olefin selectivity of iron catalysts in the fischer tropsch reaction," *Applied Catalysis*, vol. 2, no. 4-5, pp. 273–288, 1982.

[15] A. Sarkar, D. Seth, A. K. Dozier, J. K. Neathery, H. H. Hamdeh, and B. H. Davis, "Fischer-Tropsch synthesis: morphology, phase transformation and particle size growth of nano-scale particles," *Catalysis Letters*, vol. 117, no. 1-2, pp. 1–17, 2007.

[16] M. Feyzi, M. Irandoust, and A. A. Mirzaei, "Effects of promoters and calcination conditions on the catalytic performance of iron-manganese catalysts for Fischer-Tropsch synthesis," *Fuel Processing Technology*, vol. 92, no. 5, pp. 1136–1143, 2011.

[17] T. C. Bromfield and N. J. Coville, "The effect of sulfide ions on a precipitated iron Fischer-Tropsch catalyst," *Applied Catalysis A*, vol. 186, no. 1-2, pp. 297–307, 1999.

[18] C. H. Bartholomew and R. M. Bowman, "Sulfur poisoning of cobalt and iron fischer-tropsch catalysts," *Applied Catalysis*, vol. 15, no. 1, pp. 59–67, 1985.

[19] N. N. Madikizela and N. J. Coville, "A study of $Co/Zn/TiO_2$ catalysts in the Fischer-Tropsch reaction," *Journal of Molecular Catalysis A*, vol. 181, no. 1-2, pp. 129–136, 2002.

[20] J. A. Kritzinger, "The role of sulfur in commercial iron-based Fischer-Tropsch catalysis with focus on C_2-product selectivity and yield," *Catalysis Today*, vol. 71, no. 3-4, pp. 307–318, 2002.

[21] J. Li and N. J. Coville, "The effect of boron on the catalyst reducibility and activity of Co/TiO_2 Fischer-Tropsch catalysts," *Applied Catalysis A*, vol. 181, no. 1, pp. 201–208, 1999.

[22] J. Li and N. J. Coville, "Effect of boron on the sulfur poisoning of Co/TiO_2 Fischer-Tropsch catalysts," *Applied Catalysis A*, vol. 208, no. 1-2, pp. 177–184, 2001.

[23] M. Yamada, N. Koizumi, A. Miyazawa, and T. Furukawa, "Novel catalytic properties of Rh sulfide for the synthesis of methanol from $CO + H_2$ in the presence of H_2S," *Catalysis Letters*, vol. 78, no. 1–4, pp. 195–199, 2002.

[24] R. B. Anderson, *The Fischer-Tropsch Synthesis*, Academic Press, New York, NY, USA, 1984.

[25] T. Li, Y. Yang, C. Zhang et al., "Effect of manganese on an iron-based Fischer-Tropsch synthesis catalyst prepared from ferrous sulfate," *Fuel*, vol. 86, no. 7-8, pp. 921–928, 2007.

[26] H. G. Stenger and C. N. Satterfield, "Effect of liquid composition on the slurry Fischer-Tropsch synthesis. 2. Product selectivity," *Industrial & Engineering Chemistry Process Design and Development*, vol. 24, no. 2, pp. 411–415, 1985.

[27] A. M. Van der Kraan, W. L. T. M. Ramselaar, V. H. J. De Beer, G. J. Long, and F. Grandjean, *Mossbauer Spectroscopy Applied to Inorganic Chemistry*, Plenum Press, New York, NY, USA, 1989.

[28] Y. Liu, B. T. Teng, X. H. Guo et al., "Effect of reaction conditions on the catalytic performance of Fe-Mn catalyst for Fischer-Tropsch synthesis," *Journal of Molecular Catalysis A*, vol. 272, no. 1-2, pp. 182–190, 2007.

[29] C. H. Mauldin and D. E. Varnado, "Rhenium as a promoter of titania-supported cobalt Fischer-Tropsch catalysts," *Studies in Surface Science and Catalysis*, vol. 136, pp. 417–422, 2001.

[30] M. R. Housaindokht and A. Nakhaei Pour, "Study the effect of HLB of surfactant on particle size distribution of hematite nanoparticles prepared via the reverse microemulsion," *Solid State Sciences*, vol. 14, pp. 622–625, 2012.

[31] Y. Yang, H. W. Xiang, Y. Y. Xu, L. Bai, and Y. W. Li, "Effect of potassium promoter on precipitated iron-manganese catalyst for Fischer-Tropsch synthesis," *Applied Catalysis A*, vol. 266, no. 2, pp. 181–194, 2004.

[32] R. J. O'Brien, L. Xu, D. R. Milburn, Y. X. Li, K. J. Klabunde, and B. H. Davis, "Fischer-Tropsch synthesis: impact of potassium and zirconium promoters on the activity and structure of an ultrafine iron oxide catalyst," *Topics in Catalysis*, vol. 2, no. 1–4, pp. 1–15, 1995.

[33] J. A. Amelse, J. B. Butt, and L. H. Schwartz, "Carburization of supported iron synthesis catalysts," *Journal of Physical Chemistry*, vol. 82, no. 5, pp. 558–563, 1978.

[34] J. W. Niemantsverdriet, A. M. Van Der Kraan, W. L. Van Dijk, and H. S. Van Der Baan, "Behavior of metallic iron catalysts during Fischer-Tropsch synthesis studied with Mössbauer spectroscopy, X-ray diffraction, carbon content determination, and reaction kinetic measurements," *Journal of Physical Chemistry*, vol. 84, no. 25, pp. 3363–3370, 1980.

[35] R. J. Madon and W. F. Taylor, "Effect of sulfur on the Fischer-Tropsch synthesis alkali-promoted precipitated cobalt-based catalyst," *Advances in Chemistry*, vol. 178, pp. 93–111, 1979.

[36] A. Griboval-Constant, A. Y. Khodakov, R. Bechara, and V. L. Zholobenko, "Support mesoporosity: a tool for better control of catalytic behavior of cobalt supported Fischer Tropsch catalysts," *Studies in Surface Science and Catalysis*, vol. 144, pp. 609–616, 2002.